

## Evaluation of the optical axis tilt of zinc oxide films via noncollinear second harmonic generation

F. A. Bovino, M. C. Larciprete, A. Belardini, and C. Sibilia

Citation: *Applied Physics Letters* **94**, 251109 (2009); doi: 10.1063/1.3158925

View online: <http://dx.doi.org/10.1063/1.3158925>

View Table of Contents: <http://scitation.aip.org/content/aip/journal/apl/94/25?ver=pdfcov>

Published by the [AIP Publishing](#)

---

### Articles you may be interested in

[Characterization of the quality of ZnO thin films using reflective second harmonic generation](#)

*Appl. Phys. Lett.* **95**, 091904 (2009); 10.1063/1.3216848

[Second and third order nonlinear optical properties of microrod ZnO films deposited on sapphire substrates by thermal oxidation of metallic zinc](#)

*J. Appl. Phys.* **102**, 113113 (2007); 10.1063/1.2822461

[Second-harmonic performance of a -axis-oriented ZnO nanolayers on sapphire substrates](#)

*Appl. Phys. Lett.* **87**, 171108 (2005); 10.1063/1.2112199

[Second order nonlinear optical properties of zinc oxide films deposited by low temperature dual ion beam sputtering](#)

*J. Appl. Phys.* **97**, 023501 (2005); 10.1063/1.1835541

[Second harmonic generation in laser ablated zinc oxide thin films](#)

*Appl. Phys. Lett.* **73**, 572 (1998); 10.1063/1.121859

---

The banner for AIP Applied Physics Reviews features a blue background with a molecular structure of spheres and rods. On the left, there is a small image of the journal cover. The main text 'NEW Special Topic Sections' is in large white letters. Below it, 'NOW ONLINE' is in orange, followed by 'Lithium Niobate Properties and Applications: Reviews of Emerging Trends' in white. The AIP logo and 'Applied Physics Reviews' are in the bottom right corner.

**NEW Special Topic Sections**

**NOW ONLINE**  
Lithium Niobate Properties and Applications:  
Reviews of Emerging Trends

**AIP** Applied Physics Reviews

# Evaluation of the optical axis tilt of zinc oxide films via noncollinear second harmonic generation

F. A. Bovino,<sup>1</sup> M. C. Larciprete,<sup>2,a)</sup> A. Belardini,<sup>2</sup> and C. Sibilia<sup>2</sup>

<sup>1</sup>Quantum Optics Lab., Elsag-Datamat, Via Puccini 2, 16154 Genova, Italy

<sup>2</sup>Dipartimento di Energetica, Università di Roma "La Sapienza", Via A. Scarpa 16, 00161 Roma, Italy

(Received 16 April 2009; accepted 4 June 2009; published online 23 June 2009)

We investigated noncollinear second harmonic generation from zinc oxide films, grown on glass substrates by dual ion beam sputtering technique. At a fixed incidence angle, the generated signal is investigated by scanning the polarization state of both fundamental beams. We show that the map of the generated signal as a function of polarization states of both pump beams, together with the analytical curves, allows to retrieve the orientation of the optical axis and eventually, its angular tilt, with respect to the surface normal. © 2009 American Institute of Physics.

[DOI: 10.1063/1.3158925]

Second harmonic generation (SHG) is strongly dependent on the crystalline structure of the material thus offers the possibility to estimate the degree of structural order for samples produced by means of a certain deposition technique and also to retrieve information about the orientation of the optical axis. The use of two pump beams, i.e., a noncollinear scheme, was first developed by Muenchausen<sup>1</sup> and Provencher.<sup>2</sup> More importantly, both Figliozzi<sup>3</sup> and Cattaneo<sup>4</sup> have shown that this technique allows the bulk and surface responses to be distinguished. In addition, Cattaneo has also demonstrated that the technique is very useful in surface and thin-film characterization.<sup>5,6</sup>

We carried out noncollinear SHG measurements from ZnO films grown by dual ion beam sputtering. At a fixed incidence angle, the polarization state of both fundamental beams was systematically varied thus addressing all the different nonzero components of the nonlinear optical tensor.<sup>7,8</sup> The generated signal can be represented as a function of polarization states of both pump beams. The result is a *polarization map* whose pattern is characteristic of the investigated crystalline structure. We show here that this method, which does not require sample rotation, is a useful tool to put in evidence the tilt angle of the optical axis of a nonlinear optical film with respect to the surface normal, for any material whose symmetry class implies an orientation of the optical axis almost perpendicular to the surface.

Zinc oxide was chosen for the large energy gap value ( $E_g=3.37$  eV) and high nonlinear optical coefficients of both second and third order it offers. Second order nonlinear optical response has been shown in ZnO films grown by different techniques implying both high deposition temperature, as reactive sputtering<sup>9</sup> spray pyrolysis<sup>10</sup> laser ablation,<sup>11</sup> and low deposition temperature, as laser deposition,<sup>2</sup> and dual ion beam sputtering.<sup>12</sup> Generally, the reduced deposition temperature results in polycrystalline films, where the average orientation of crystalline grains, along with the resulting optical axis, can be tilted with respect to the ideal crystal, i.e., normal to sample surface.

ZnO crystalline structure, i.e., wurtzite, belongs to the noncentrosymmetric point group symmetry 6mm with a hex-

agonal primary cell. If the optical axis is normal to the sample surface and corresponds to the direction of the  $z$ -axis, the second order susceptibility tensor  $\tilde{d}$ , displays three nonvanishing components<sup>13</sup> along with the piezoelectric contraction,  $d_{15}=d_{24}$ ,  $d_{31}=d_{32}$ , and  $d_{33}$ . Assuming Kleinmann symmetry<sup>14</sup> they reduce to two independent coefficients,  $d_{15}=d_{24}=d_{31}=d_{32}$  and  $d_{33}$ . Furthermore, for an ideal wurtzite structure the nonzero elements are related to each other via the  $d_{33}=-2d_{31}$ .<sup>15</sup> If, on the other hand, the optical axis is tilted, with respect to the surface normal, a rotation must be applied to the nonlinear optical tensor, which is equivalent to the introduction of other nonvanishing terms in  $\tilde{d}$ .

Zinc oxide films, 400 nm thick, were deposited by means of a dual ion beam sputtering system onto 1 mm thick silica substrates. X-ray diffraction (XRD) profiles show a peak in the  $\theta/2\theta$  curves located at  $2\theta\sim 34.4^\circ$ , originated from the 0002 planes of ZnO, as reported in Fig. 1, indicating that the films are polycrystalline with the  $c$ -axis preferentially oriented about the surface normal.<sup>16</sup>

SHG measurements were carried out by means of a noncollinear scheme working in transmission. The output of a mode-locked Ti:Sapphire laser system tuned at  $\lambda=830$  nm (76 MHz repetition rate, 130 fs pulse width) was split into two beams of comparable power, while the temporal overlap of the incident pulses was controlled with an external delay line. The polarization of both beams was varied with two

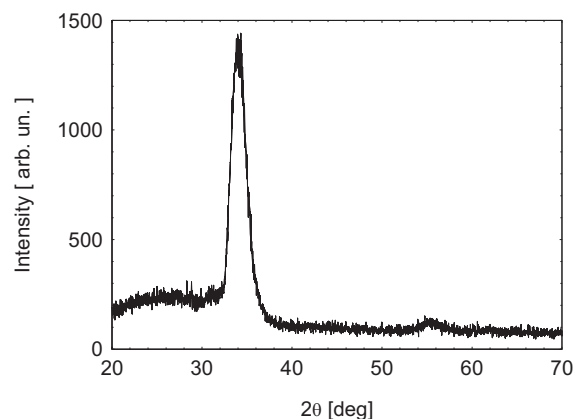


FIG. 1. XRD profiles of the ZnO films, 400 nm thick, grown by dual ion beam sputtering onto 1 mm glass substrate.

<sup>a)</sup>Author to whom correspondence should be addressed. Electronic mail: mariacristina.larciprete@uniroma1.it.

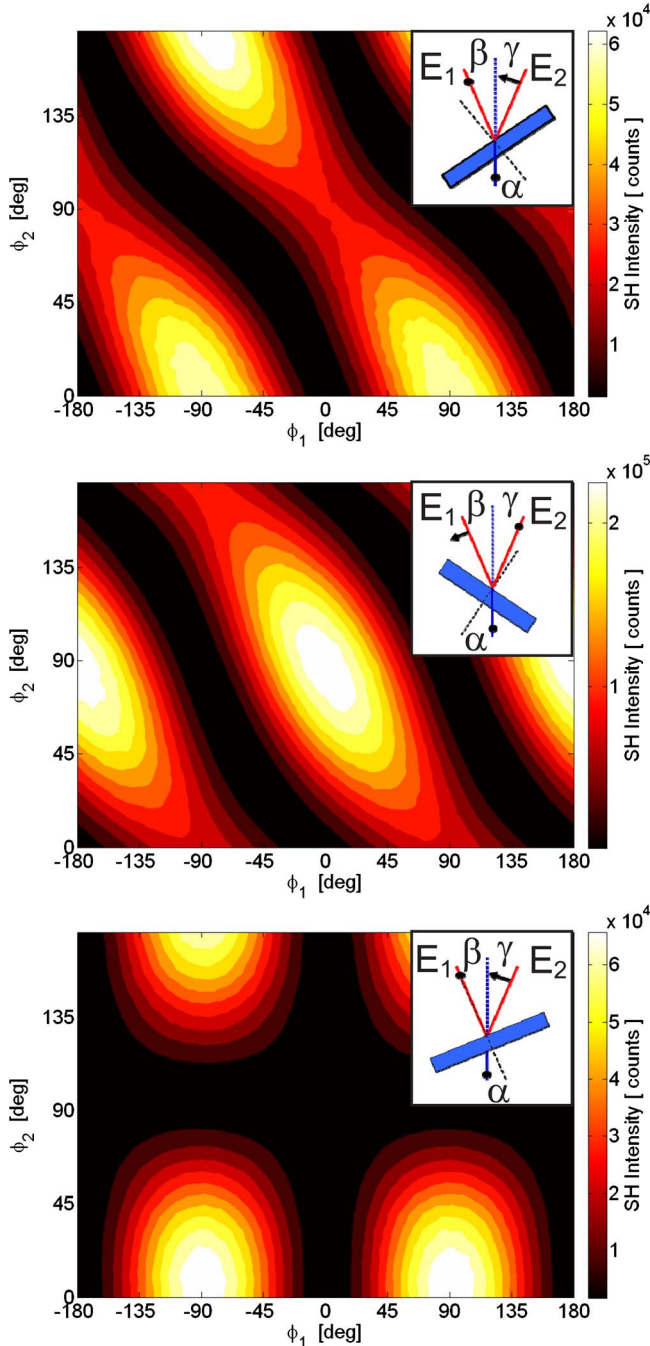


FIG. 2. (Color online) SH signal as a function of the polarization angle of the first pump beam ( $\phi_1$ ) and the second pump beam ( $\phi_2$ ). Sample rotation angle was fixed to (a)  $\alpha=35^\circ$ , (b)  $\alpha=-35^\circ$ , and (c)  $\alpha=9^\circ$ , respectively. Polarization state of the analyzer is set to  $\hat{S}$ , i.e.,  $\phi=90^\circ$ . The insets show the condition for the polarization states of the two pump beams to get the absolute maxima.

identical rotating half-wave plates, and the two collimating lenses, 150 mm focal length, were placed thereafter. The sample was placed onto a motorized stage, allowing the variation of the sample rotation angle,  $\alpha$ . The pump beams, laying in the same plane of incidence, were sent to intersect in the focus region with an angle of  $\beta=9^\circ$  and  $\gamma=-9^\circ$ , measured with respect to  $\alpha=0^\circ$  (see the insets in Fig. 2). Thus, for a given  $\alpha \neq 0^\circ$ , the corresponding incidence angles result to be  $\alpha_1=\alpha-\beta$  and  $\alpha_2=\alpha-\gamma$ , respectively.

The interaction of two incident beams linearly polarized, tuned at  $\omega_1$  and  $\omega_2$ , with a noncentrosymmetric material, produces a nonlinear polarization oscillating at the frequency

$\omega_1 + \omega_2$ . Given the wave vectors' conservation law  $\vec{k}_{\omega_1} + \vec{k}_{\omega_2} = \vec{k}_{\omega_1 + \omega_2}$ , the generated beam is emitted nearly along the bisector of the aperture angle between the two pump beams. This beam was collected with an objective and focused on to a monomodal optical fiber coupled with a photon counting detector. Here, a set of optical low pass filters was used to further suppress any residual light at  $\omega_1$  and  $\omega_2$ , while an analyzer allowed to select the desired SH polarization state.

The analytical expression of the effective susceptibility,  $d_{\text{eff}}$  (Ref. 17) is significantly simplified for particular crystalline symmetries. Specifically, for the ZnO crystalline structure, considering four combination of polarization states of the two pump beams,  $\hat{p}_{\omega_1}-\hat{p}_{\omega_2}$ ,  $\hat{s}_{\omega_1}-\hat{s}_{\omega_2}$ ,  $\hat{p}_{\omega_1}-\hat{s}_{\omega_2}$ , and  $\hat{s}_{\omega_1}-\hat{p}_{\omega_2}$ , four different expressions for  $d_{\text{eff}}$  are allowed, depending on the SH polarization state, i.e., either  $\hat{P}$  or  $\hat{S}$

$$\begin{aligned}
 d_{\text{eff}}^{pp \rightarrow P} &= -\cos(\alpha_{2\omega})d_{24}[\cos(\alpha'_1)\sin(\alpha'_2) + \cos(\alpha'_2)\sin(\alpha'_1)] \\
 &\quad + \sin(\alpha_{2\omega})[-d_{32}\cos(\alpha'_1)\cos(\alpha'_2) \\
 &\quad - d_{33}\sin(\alpha'_2)\sin(\alpha'_1)], \\
 d_{\text{eff}}^{ss \rightarrow P} &= -\sin(\alpha_{2\omega})d_{31}, \\
 d_{\text{eff}}^{ps \rightarrow S} &= -d_{15}\sin(\alpha'_1), \\
 d_{\text{eff}}^{sp \rightarrow S} &= -d_{15}\sin(\alpha'_2),
 \end{aligned} \tag{1}$$

where  $\alpha'_1$  and  $\alpha'_2$  are the internal propagation angles and  $\alpha_{2\omega}$  is the angle of emission of the SHG inside the crystal. For pump beams linearly polarized with two generic polarization angles,  $\phi_1$  and  $\phi_2$ , the  $d_{\text{eff}}$  can be still calculated as  $d_{\text{eff}} = \vec{d}\vec{E}_1(\phi_1, \alpha_1) \cdot \vec{E}_2(\phi_2, \alpha_2)$ .

The experimental measurements were obtained by rotating the two half-wave plates, in the range  $-180^\circ$ – $+180^\circ$  for pump beam 2 and  $0^\circ$ – $180^\circ$  for pump beam 1. Different  $\alpha$  as well as polarization state of generated beam were investigated, although we here report only the measurements of  $\hat{S}$  polarized SH signal for the sake of brevity.

When the analyzer is set to  $\hat{S}$ -polarization, i.e.,  $\phi=90^\circ$ , the maxima of SH signal occur when the two pump beams have crossed polarization. The last two equations in Eq. (1) show that this condition is not symmetrical for positive and negative rotation angles  $\alpha$ , since the position of the two beams, differently polarized, with respect to the sample surface is not symmetrical. When  $\alpha=35^\circ$  [Fig. 2(a)], the absolute maxima take place when pump 1 is  $\hat{s}$ -polarized and pump 2 is  $\hat{p}$ -polarized, i.e.,  $\phi_1$  equal to  $\pm 90^\circ$  and  $\phi_2$  to either  $0^\circ$  or  $180^\circ$ , while relative maxima occur in the reverse situation, that is pump 1 is  $\hat{p}$ -polarized and pump 2  $\hat{s}$ -polarized. According with the theoretical model, we found the opposite behavior when the rotation angle  $\alpha$  is set to  $-35^\circ$ , as shown in Fig. 2(b), thus the absolute and relative maxima appear to be inverted with respect to the previous situation. For both  $\alpha$  values, when the two pumps are equally polarized, either  $\hat{s}$  or  $\hat{p}$ , the nonlinear optical tensor do not allow  $\hat{S}$ -polarized SH signal.

Experimental plots obtained for  $\alpha=9^\circ$  are shown in Fig. 2(c). In this particular condition, the absolute maxima still require  $\hat{s}$ -polarization for pump 1 and  $\hat{p}$ -polarization for pump 2 (i.e.,  $\phi_1 = \pm 90^\circ$  and  $\phi_2$  equal to either  $0^\circ$  or  $180^\circ$ ), whereas the relative maxima totally disappeared. This peculiarity can be reasonably explained considering that  $\alpha=9^\circ$



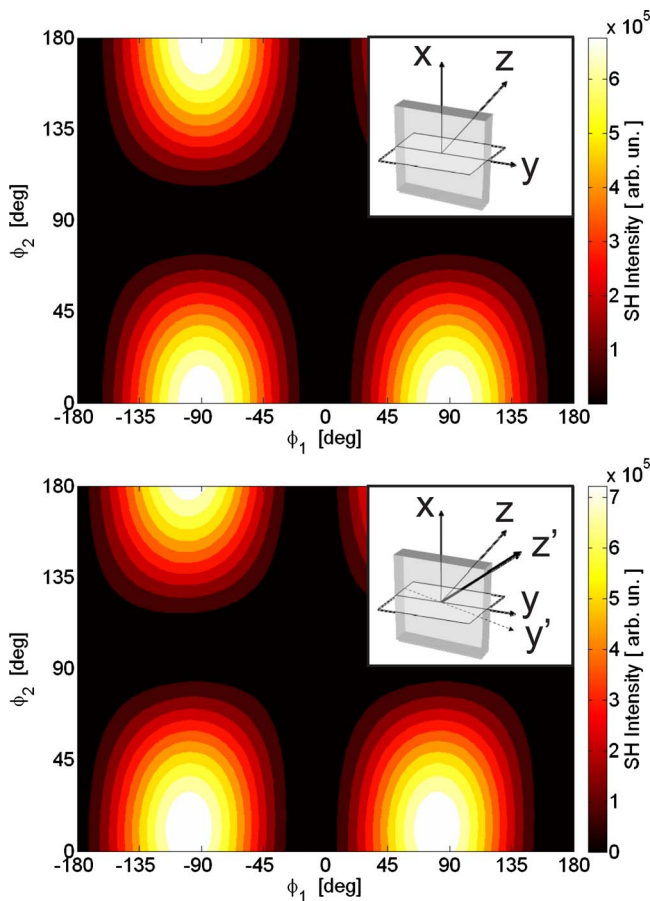


FIG. 3. (Color online) Theoretically calculated curves of  $\hat{S}$ -polarized SH signal as a function of the polarization angle of the first pump beam ( $\phi_1$ ) and the second pump beam ( $\phi_2$ ), calculated for the optical axis (a) normal to the sample surface and (b) tilted about the  $x$ -axis of  $2^\circ$ . Sample rotation angle is  $\alpha=9^\circ$ . Thick arrow in the insets represents the optical axis orientation.

corresponds to a situation such that the pump beam 1 is normally incident onto the sample, as can be seen from the inset. For an anisotropic uniaxial crystal with its optical axis perpendicular to sample surface, a normally incident wave always experiences the ordinary refractive index, whatever its polarization angle, thus pump beam 1 always corresponds to an  $\hat{s}$ -polarized beam. As a consequence for  $\alpha=9^\circ$ , the condition to get a relative maximum, i.e.,  $\hat{p}$ -polarization for pump 1 and  $\hat{s}$ -polarization for pump 2, is never fulfilled, being replaced with the condition equivalent to two pumps both having  $\hat{s}$ -polarization. This combination does not allow  $\hat{S}$ -polarized SH signal, thus the relative maxima disappear. Moreover, we found out that the experimental configuration where one of the pump beams is normally incident onto the sample is particularly sensitive to the orientation of the optical axis.

The experimental curves were fully reconstructed using the expression for the effective second order optical nonlinearity in noncollinear scheme, assuming the Kleinmann symmetry rules. Dispersion of both the ordinary and extraordinary refractive indices of ZnO,  $n(\lambda)$  was taken from Ref. 3. We show in Fig. 3(a) the calculated curve for  $\alpha=9^\circ$ , when the optical axis is assumed to be perpendicular to sample surface. If compared with the theoretical one, the experimental curve appears to be shifted toward higher  $\phi_2$ . This differ-

ence suggests that the optical axis may be averagely tilted with respect to the surface normal. This is a reasonable assumption, taking into account the low temperature deposition technique which was employed.

An angular tilt of the optical axis was then introduced in the analytical model through a rotation matrix, applied on the  $d_{\text{eff}}$ . The rotation produces the arising of new terms in the nonlinear optical tensor. In Fig. 3(b) we show the new curve, calculated for a tilt of  $2^\circ$  around the  $x$ -axis, as shown in the inset. The obtained theoretical curve displays the same  $\phi_2$ -shift evidenced in the experimental curves, thus indicating that the film has a partially oriented polycrystalline structure, as shown by the x-ray analysis, but the orientation of the optical axis is not exactly normal to the film surface. Similar curves were calculated by tilting the optical axis, around the other two reference axes. For the investigated crystalline symmetry group, 6mm, a rotation about the  $z$ -axis do not produce any change in the  $d_{\text{eff}}$ . On the other side, a rotation about the  $y$ -axis produce an analogous shift in the  $\hat{S}$ -polarized SH pattern, but also a modification in the  $\hat{P}$ -polarized SH pattern which was not compatible with the corresponding experimental curves.

In conclusion, we investigated second order nonlinear optical properties of ZnO films deposited by dual ion beam sputtering, with a noncollinear experimental setup. We show that, from the contour plot of the generated signal as a function of polarization states of both pump beams, important information on the crystalline structure of the films can be deduced. The polarization scanning method adopted is a valid and sensitive tool to probe the orientation of the optical axis and to evidence possible angular tilt with respect to surface normal.

M. Centini is acknowledged for helpful discussion. ZnO films were grown with F. Sarto at the Division of Advanced Physics Technologies of ENEA (Roma, Italy).

<sup>1</sup>R. E. Muenchausen, R. A. Keller, and N. S. Nogar, *J. Opt. Soc. Am. B* **4**, 237 (1987).

<sup>2</sup>P. Provencher, C. Y. Côté, and M. M. Denariez-Roberge, *Can. J. Phys.* **71**, 66 (1993).

<sup>3</sup>P. Figliozzi, L. Sun, Y. Jiang, N. Matlis, B. Mattern, M. C. Downer, S. P. Withrow, C. W. White, W. L. Mochán, and B. S. Mendoza, *Phys. Rev. Lett.* **94**, 047401 (2005).

<sup>4</sup>S. Cattaneo and M. Kauranen, *Phys. Rev. B* **72**, 033412 (2005).

<sup>5</sup>S. Cattaneo and M. Kauranen, *Opt. Lett.* **28**, 1445 (2003).

<sup>6</sup>S. Cattaneo, E. Vuorimaa, H. Lemmetyinen, and M. Kauranen, *J. Chem. Phys.* **120**, 9245 (2004).

<sup>7</sup>J. Jerphagnon and S. K. Kurtz, *J. Appl. Phys.* **41**, 1667 (1970).

<sup>8</sup>D. Faccio, V. Pruneri, and P. G. Kazansky, *Opt. Lett.* **25**, 1376 (2000).

<sup>9</sup>G. Wang, G. T. Kiehne, G. K. Wong, J. B. Ketterson, X. Liu, and R. P. H. Chang, *Appl. Phys. Lett.* **80**, 401 (2002).

<sup>10</sup>U. Neumann, R. Grunwald, U. Griebner, G. Steinmeyer, and W. Seeber, *Appl. Phys. Lett.* **84**, 170 (2004).

<sup>11</sup>H. Cao, J. Y. Wu, H. C. Ong, J. Y. Dai, and R. P. H. Chang, *Appl. Phys. Lett.* **73**, 572 (1998).

<sup>12</sup>M. C. Larciprete, D. Passeri, F. Michelotti, S. Paoloni, C. Sibilia, M. Bertolotti, A. Belardini, F. Sarto, F. Somma, and S. Lo Mastro, *J. Appl. Phys.* **97**, 023501 (2005).

<sup>13</sup>A. Yariv, *Optical Electronics*, 4th ed. (Saunders, Philadelphia, 1991).

<sup>14</sup>V. G. Dmitriev, G. G. Gurzadyan, and D. N. Nikogosyan, *Handbook of Nonlinear Optical Crystals* (Springer, New York, 1997).

<sup>15</sup>B. F. Levine, *Phys. Rev. B* **7**, 2600 (1973).

<sup>16</sup>K. S. Weisenrieder and J. Muller, *Thin Solid Films* **300**, 30 (1997).

<sup>17</sup>P. A. Franken and J. F. Ward, *Rev. Mod. Phys.* **35**, 23 (1963).